Research Square

Preprints are preliminary reports that have not undergone peer review.
They should not be considered conclusive, used to inform clinical practice,
or referenced by the media as validated information.

Experimental study on shear creep and microscopic damage of sandstone discontinuities under high temperatures

Fengrui Zhang
Huai'an University
Wei Yin
Huai'an University
Hui Wang
Huai'an University
Xuewen Zheng
Huai'an University
Haopeng Jiang
hoperjiang_2017@126.com
Huai'an University

Research Article

Keywords: High temperature, Sandstone discontinuities, Shear creep, SEM, NMR

Posted Date: June 19th, 2026

DOI: https://doi.org/10.21203/rs.3.rs-9822970/v1

License: This work is licensed under a Creative Commons Attribution 4.0 International License.
Read Full License

Additional Declarations: No competing interests reported.

Experimental study on shear creep and microscopic damage of sandstone discontinuities under high temperatures

Fengrui Zhang[a], Wei Yin, HuiWang[a], Xuewen Zheng[a], Haopeng Jiang[a*]

[a] *Faculty of Transportation Engineering, Huai'an University, Huaian 223003, China*

Abstract

Investigating the shear creep characteristics of sandstone discontinuities and the mechanisms of their microscopic thermal damage under high temperatures is of paramount importance for the long-term stability analysis of deep rock mass engineering. First, sandstone discontinuity specimens possessing identical surface morphology were fabricated using 3D scanning and engraving techniques. Then, shear creep tests were performed under different high-temperature conditions to investigate the effects of temperature on the creep deformation, creep rate, and long-term strength of the discontinuities. The combined utilization of SEM and NMR tests was employed to further investigate the influence of high temperatures on the evolution of microcracks and pore structures in sandstone, thus elucidating the microscopic thermal damage mechanisms. The results indicate that: (1) With increasing temperature, the specimens exhibited a continuous increase in creep deformation and creep rate, accompanied by a gradual reduction in creep duration and long-term strength. Elevated temperature promotes the development of nonlinear creep characteristics in the discontinuities. (2) High temperature facilitates the development of pores and microcracks within the specimen, generating numerous surface cracks. Furthermore, the internal micro-pores and small pores gradually grow and interconnect, forming medium-sized and large pores. This evolution enhances the overall pore connectivity of the rock, which in turn leads to the deterioration of its creep mechanical properties. (3) At elevated temperatures, sandstone undergoes a series of physicochemical reactions, including dehydration, quartz phase transition, mineral oxidation, and chemical bond breakage. These reactions induce the formation of intergranular cracks, transgranular cracks, and detachment defects among mineral particles. The high temperature promotes the proliferation and propagation of these

*Corresponding author.

E-mail address: hoperjiang_2017@126.com

cracks, resulting in aggravated thermal damage. The findings of this study can provide a reference for rock mass construction, remediation, and surrounding rock stability analysis in high-temperature environments.

Keywords: High temperature; Sandstone discontinuities; Shear creep; SEM; NMR

1. Introduction

The ongoing advancement of rock mass engineering into deeper strata, driven by mineral resource extraction, geothermal development, and geological disposal of nuclear waste, has led to a growing number of projects involving high temperatures. This trend presents increasingly complex engineering difficulties, with the high-temperature issue now emerging as a critical bottleneck constraining the sustainable development of deep rock engineering (Zhou et al. 2024; Shen et al. 2025; Hu et al. 2024; Fan et al. 2024). Due to increased burial depth, rock masses persist in complex environments characterized by high geotemperature and high in-situ stress. Their instability and failure typically do not occur immediately upon excavation but manifest as creep-induced instability after a significant duration, thereby critically impacting project safety and long-term stability (Yang et al. 2023; Li et al. 2024; Zhao et al. 2025). Consequently, investigating the evolution of the creep mechanical properties of rocks under high temperatures is imperative.

Considerable research efforts have been devoted by numerous scholars to investigating the creep mechanical properties of rocks under high temperatures (Liang et al. 2022; Xu et al. 2024; Tounsi et al. 2023). Through triaxial creep tests coupled with acoustic emission monitoring at elevated temperatures, Dong et al. (2023) revealed that high temperatures shorten the transient creep stage, accelerate the steady-state creep rate, and induce an earlier transition into the dilatant stage in rock salt. Jiang et al. (2025) developed a nonlinear creep model for layered rock that incorporates the coupled damage induced by high-temperature loading, and validated its accuracy through creep tests. Yang et al. (2021) conducted creep and permeability tests on sandstone under loading-unloading cycles at high temperatures. They identified a critical thermal damage threshold at 500°C, noting that the resultant thermal microcracks significantly enhance rock permeability and alter the creep mechanism. Zhao et al. (2025) and Yang et al. (2024) investigated the effects of high temperature on the evolution

of creep damage properties and microstructure in rocks. Pan et al. (2025) analyzed the variations in creep strain, creep rate, long-term strength, porosity, and acoustic emission characteristics of rocks under high temperatures, and established a nonlinear creep model that incorporates thermal effects. Li et al. (2024) conducted triaxial compression creep tests on rocks under high temperatures and dynamic disturbances. They observed that the granite creep curve exhibited decelerating, steady-state, accelerating, and disturbance characteristics, and subsequently developed a fractional-order nonlinear creep model. Meng et al. (2025) proposed a modified Nishihara model that incorporates thermal damage and bedding plane orientation. The model's validity was confirmed through triaxial creep tests, demonstrating its capability to overcome the limitations of conventional models in describing the accelerated creep stage. Zhang et al. (2024) and Wang et al. (2014) established a visco-elasto-plastic creep damage model capable of reflecting the entire rock creep process, taking into account the coupled effects of temperature and stress on rock creep performance. Collectively, these experimental studies reveal that temperature induces thermal damage in rocks, and that exposure to high temperatures leads to significant alterations in their creep mechanical propertie

The aforementioned are predominantly based on homogeneous rocks under high temperatures, with limited consideration given to the influence of rock discontinuity. In practical engineering contexts, rock masses are intersected by abundant discontinuities. Cracking or shear deformation within the rock mass often initiates along these discontinuities, which represent planes of relative mechanical weakness, thereby playing a decisive role in the overall stability of the rock mass (Pan et al. 2022; Feng et al. 2024; Xu et al. 2024; Yu et al. 2024). Under high temperatures, the creep mechanical behavior of rock discontinuities becomes considerably more complex. Their deformation characteristics and failure modes differ significantly from those observed in intact rock. Consequently, investigating the creep mechanical properties of rock discontinuities under high temperatures is of paramount importance for practical engineering applications.

Based on this, the present study employed 3D scanning and engraving techniques to replicate sandstone discontinuity specimens with identical surface morphology. Shear creep tests were subsequently conducted on these specimens after exposure to various high

temperatures (20, 200, 400, 600, 800°C). Integrated with scanning electron microscopy (SEM) and nuclear magnetic resonance (NMR) tests, this research elucidates the evolution of creep mechanical characteristics and the underlying microscopic damage mechanisms in sandstone discontinuities following thermal treatment. The findings provide experimental evidence and theoretical guidance for stability control in deep underground engineering projects involving high-temperature rock masses.

2. Specimen preparation and experimental program

2.1 Specimen preparation

The experimental study utilized red sandstone, sourced from a mining area in Jining City, Shandong Province, China. The sandstone exhibits a reddish-brown color, dense lithology, absence of apparent joints, and a fine sandy structure. X-ray diffraction (XRD) analysis indicates that the primary mineral composition of the red sandstone is 67% quartz, 22% feldspar, 9% kaolinite, and 2% hematite, as shown in Fig. 1.

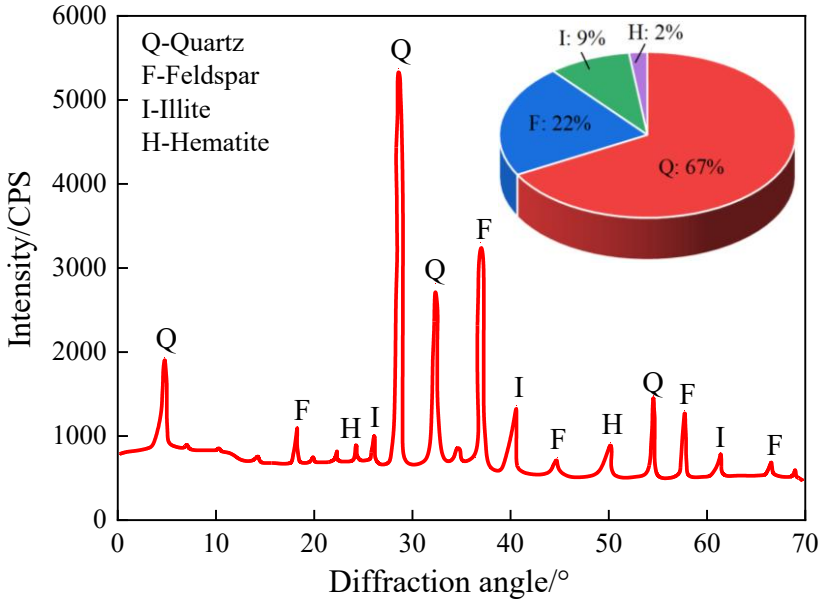


Fig. 1. Mineral composition of red sandstone

The rock blocks obtained on-site were processed into two specimen geometries: 100mm×100mm×100mm cubic specimens and Φ50mm×100mm standard cylindrical specimens. Basic physico-mechanical properties were determined using the standard cylindrical specimens, and the corresponding mechanical parameters are summarized in Table 1.

Table 1. Basic physico-mechanical parameters of red sandstone

Density (g/cm^3)	Elastic Modulus/GPa	Poisson's ratio	Porosity/%	P-wave velocity (km/s)	Uniaxial compressive strength/MPa
2.34	6.9	0.27	8.52	2.57	49.82

Due to the complex morphology and significant variability of natural discontinuities, a substantial number of replicated discontinuity specimens with identical lithology, surface morphology, and mechanical properties are required to mitigate the influence of inherent discreteness and maintain relative homogeneity. To this end, this study employed a rock discontinuity reconstruction method based on 3D scanning and engraving technology to prepare red sandstone discontinuity specimens for the subsequent shear creep tests.

The specific procedure for preparing red sandstone discontinuity specimens is outlined as follows: First, a direct shear test was performed on a 100mm×100mm×100mm red sandstone cube. The test was carried out under a constant normal stress of 10MPa in displacement-control mode, with a shear rate of 0.005mm/s, to generate a corresponding natural rock discontinuity surface. Subsequently, the generated natural rock discontinuity surface was scanned using a 3D scanner to acquire a digital surface model that precisely replicates its morphology. This surface model data was then imported into a 3D engraving machine and converted into an engraving path map interpretable by the machine system. Finally, a pre-prepared red sandstone specimen measuring 100mm×100mm×50mm was secured onto the engraving workstation. Upon equipment activation, the 3D engraving machine automatically and intelligently executed the discontinuity engraving process. After the lower half of the discontinuity specimen was completed, the engraving path was reversed. By replacing it with a new pre-prepared red sandstone specimen and repeating the aforementioned procedures, the upper half was fabricated, as shown in Fig. 2.

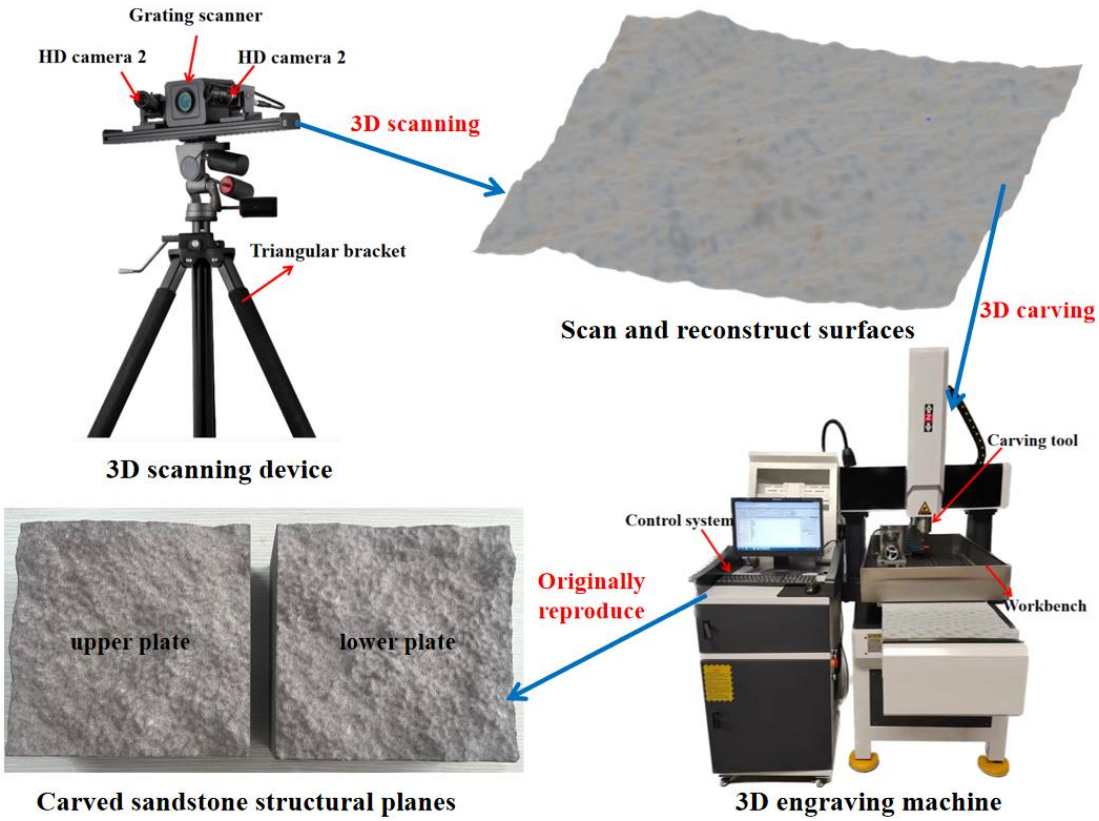


Fig. 2. Production process of red sandstone discontinuities

This method enables the efficient replication of specimens that share the same lithology, surface morphology, and mechanical properties as the natural rock discontinuity, as shown in Fig. 3. Observation confirms that the engraved red sandstone discontinuities exhibit highly consistent surface morphology, making them suitable for investigating the shear creep behavior of discontinuities.



Fig. 3. Red sandstone discontinuity specimens

2.2 Experimental Program

The processed red sandstone discontinuity specimens were subjected to thermal treatment using a high-temperature chamber electric furnace, which can reach a maximum temperature of 1200°C. To minimize the influence of heating rate on the mechanical properties of the specimens, the heating rate was set to 5°C/min. Four target temperature levels were established: 200, 400, 600, and 800 °C. Upon reaching the target temperature, a 2h dwell time was maintained to ensure a uniform temperature field throughout the specimen. After the heating process, the specimens were removed from the electric furnace and allowed to cool naturally at ambient room temperature. The heating protocol is shown in Fig. 4.

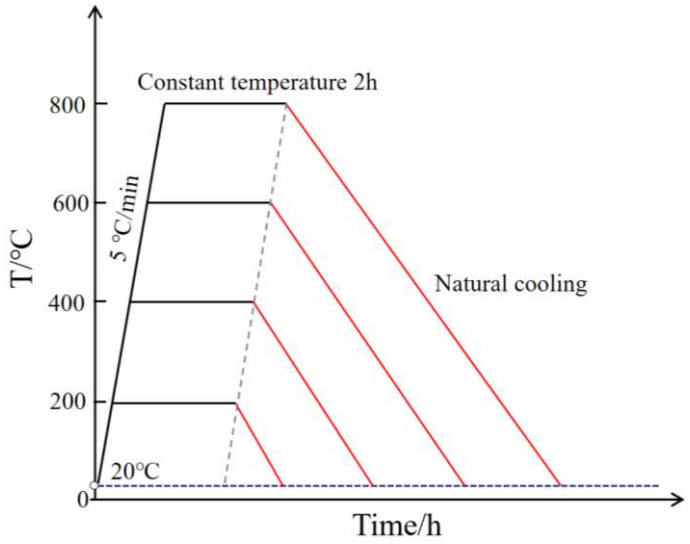
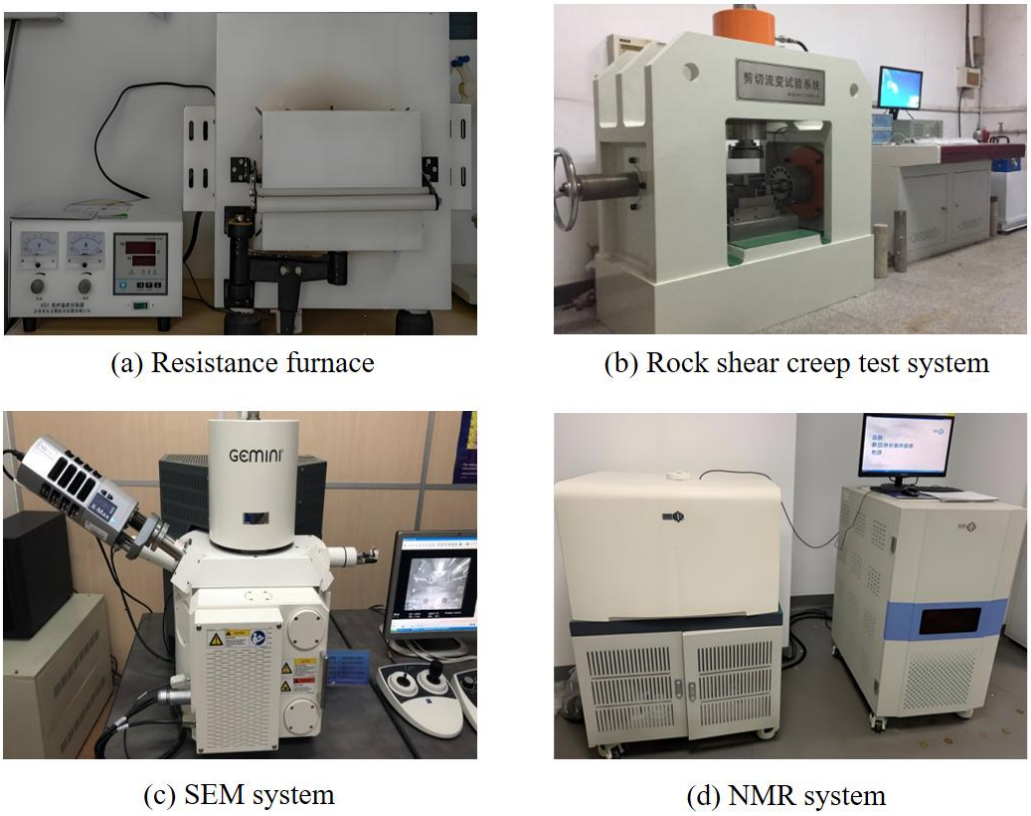


Fig. 4. Heating Protocol

Shear creep tests were conducted using a rock shear rheological testing system. This system features a fully digital computer-automated control system, with a load capacity range of 50-2000kN, a measurement accuracy≤±0.5%FS, and a maximum displacement of 50mm. The testing employed a multi-stage loading procedure. Based on in-situ stress measurements from deep boreholes in the mining area, the normal stress was set to 10MPa. The shear stress levels for the creep test were determined based on the instantaneous shear strength of the specimens. The multi-stage loading scheme consisted of 4-6 stages, with each stage incremented by a shear stress of 0.5MPa. The loading rate was set at 0.1MPa/min. Upon reaching each predetermined load level, it was maintained constant for 48h. The subsequent loading stage was initiated only after the specimen's displacement rate stabilized below 0.01mm/h over the final period of this 48-hour hold. This multi-stage loading process

continued progressively until specimen failure occurred. Throughout the entire test, stress, displacement, and time data were continuously recorded. The experimental program is summarized in Table 2. Finally, SEM and NMR techniques were employed to qualitatively and quantitatively analyze the microscopic thermal damage characteristics of the sandstone. The experimental setup is shown in Fig. 5.



(a) Resistance furnace (b) Rock shear creep test system

(c) SEM system (d) NMR system

Fig. 5. Experimental Setup

Table 2. Test scheme

Sample number	*T*/°C	Normal stress/MPa	Shear stress/MPa
T-1	20	10	Initial 0.5MPa, each level loading 0.5MPa, until failure
T-2	200		
T-3	400		
T-4	600		
T-5	800		

3. Analysis of shear creep test results

3.1 Creep deformation characteristics

Fig. 6 shows the shear creep curves of sandstone discontinuity specimens under high temperatures. It can be observed that each loading stage induced an instantaneous shear displacement. The magnitude of this instantaneous displacement progressively increased with temperature: at 20°C, the initial instantaneous shear displacement was 0.269mm, while at 200°C, 400°C, 600°C, and 800°C, the corresponding displacements were 0.435mm, 0.647mm, 0.898mm, and 1.159mm, respectively. With increasing shear stress levels, the shear creep displacement of the specimens gradually increased, exhibiting decelerating creep characteristics followed by steady-state creep. Furthermore, as temperature rose, the specimens displayed larger creep displacements and more pronounced creep phenomena. Upon application of the final load stage, distinct accelerating creep characteristics emerged, where both the creep rate and displacement progressively increased with time until specimen failure occurred.

The shear creep process of the specimens primarily comprised four distinct stages: instantaneous deformation, decelerating creep, steady-state creep, and accelerating creep. Under the final loading stage, the failure stress of the specimens progressively decreased with increasing temperature. The failure stress was 3MPa at 20°C, whereas it measured 2.5MPa, 2.5MPa, 2MPa, and 2MPa at 200°C, 400°C, 600°C, and 800°C, respectively.

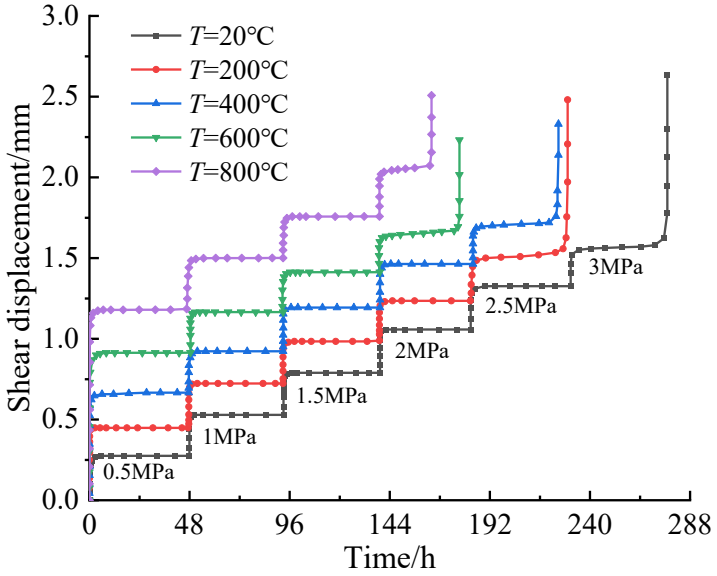


Fig. 6. Shear creep curves of the specimens under high temperatures

To further investigate the coupled effects of temperature and shear stress on the shear creep behavior of the specimens, the relationship between shear creep displacement and

temperature under different shear stress levels was plotted, as shown in Fig. 7. Under identical shear stress, the shear creep displacement of the specimen progressively increases with temperature. The magnitude of this increase becomes more pronounced at higher temperatures. The extent of the displacement increase is greater at high shear stress levels compared to low shear stress levels. For instance, under shear stress 0.5MPa, the creep displacement is 0.275mm at 20°C and rises to 1.185mm at 800°C, representing an increase of 0.91mm. In contrast, under shear stress 2MPa, the displacement increases from 1.123mm at 20°C to 2.512mm at 800°C, corresponding to a larger increase of 1.389mm.

Furthermore, at a constant temperature, the shear creep displacement of the specimen exhibits a nonlinear increasing trend with rising shear stress. For example, at 600°C, the shear creep displacement increases from 0.913mm under the first load level to 2.034mm under the final load level.

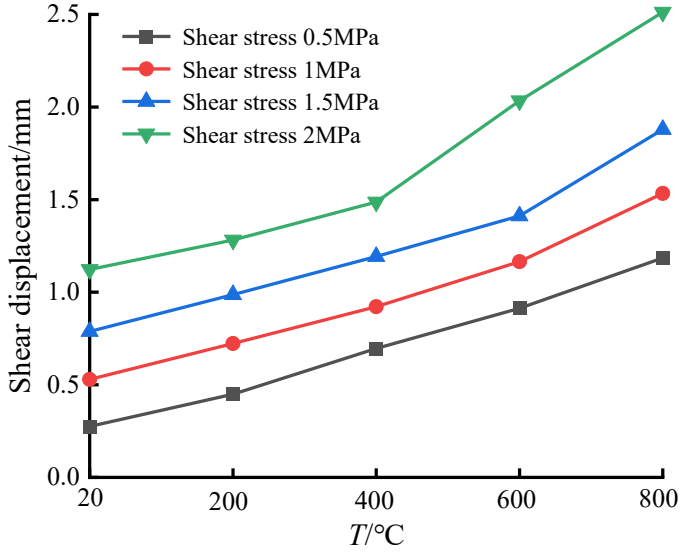


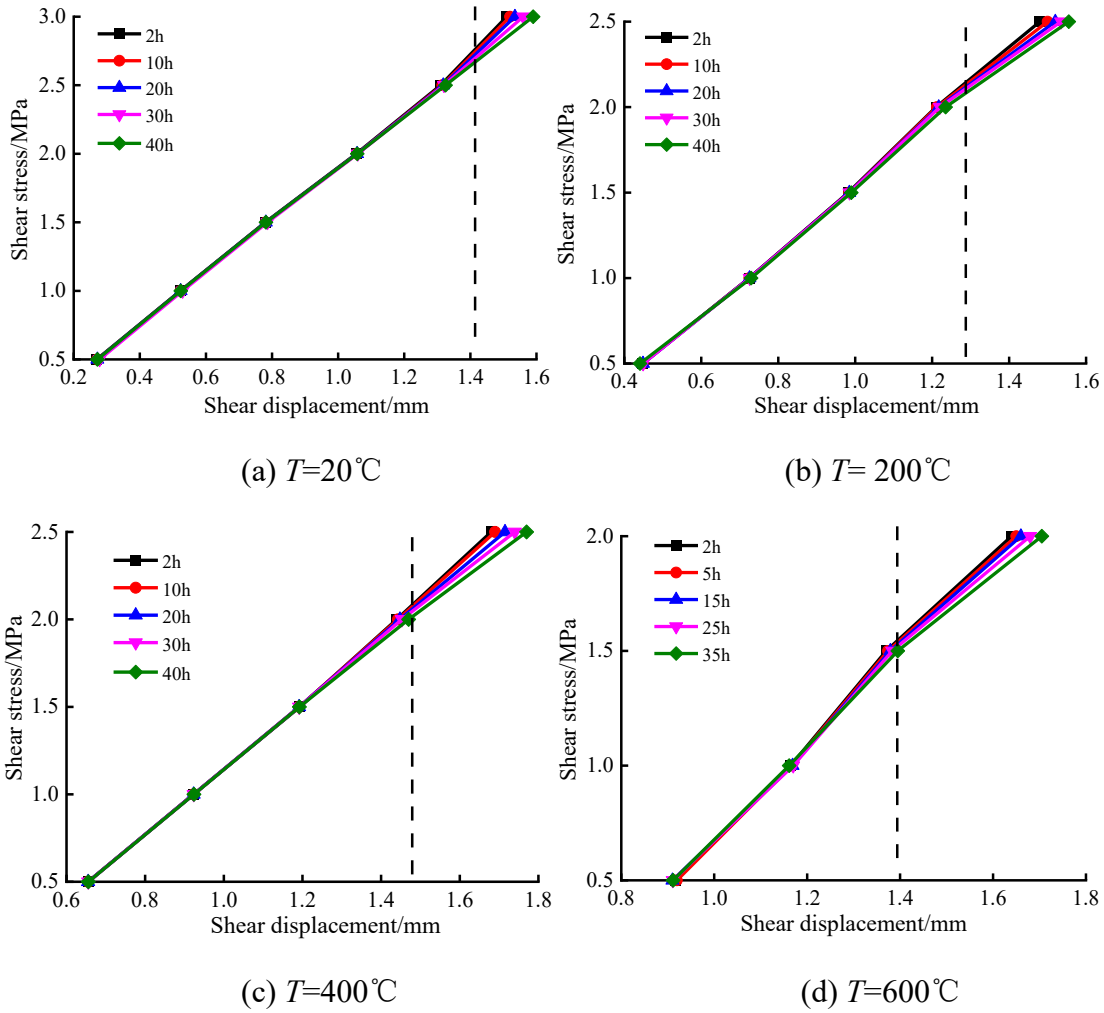
Fig. 7. Variation of specimen shear displacement with temperature under different shear stress levels

3.2 Isochronous stress-strain curves

Using the principle of superposition, the shear creep curves were processed to obtain the isochronous stress-strain curves of the specimens under high temperatures, as shown in Fig. 8. The isochronous stress-strain curves of the discontinuities at different times exhibit similar shapes. As time increases, the slope of these curves gradually decreases. At any given time, with increasing shear stress, the secant modulus of the isochronous stress-strain curve

continuously decreases, which progressively reveals the nonlinear characteristics of the discontinuity creep. These features are illustrated in Fig. 8(a) and 8(b).

Furthermore, the rate of change in the slope of the isochronous stress-strain curves increases significantly with rising temperature, as shown in Fig. 8(c) and 8(d), indicating more pronounced nonlinear creep characteristics of the discontinuities. This phenomenon can be attributed to the fact that elevated temperature intensifies slip and damage along the discontinuities, leading to continuous strength degradation and increased deformation, thereby promoting the development of nonlinear creep behavior.



(a) T=20℃ (b) T= 200℃

(c) T=400℃ (d) T=600℃

Fig. 8. Isochronous stress-strain curves of the specimens under high temperatures

3.3 Creep Rate Curves

Fig. 9 shows the relationship between the steady-state creep rate and shear stress for specimens under high temperatures. The steady-state creep rate is influenced not only by the magnitude of the shear stress but also by the temperature. Under the same temperature

condition, the steady-state creep rate exhibits a nonlinear increasing trend with rising shear stress, which conforms to an exponential function relationship. For instance, at 200°C, the steady-state creep rate increases from 1.86×10^{-4}mm/h under the first load level to 10.16×10^{-4}mm/h under the final load level. Under identical shear stress, the steady-state creep rate of the specimen progressively increases with temperature. For example, at shear stress 1.5MPa, the steady-state creep rate is 1.51×10^{-4}mm/h at 20°C. As the temperature rises to 200°C, 400°C, 600°C, and 800°C, the corresponding creep rates are 1.93×10^{-4}mm/h, 2.35×10^{-4}mm/h, 4.28×10^{-4}mm/h, and 5.32×10^{-4}mm/h, respectively.

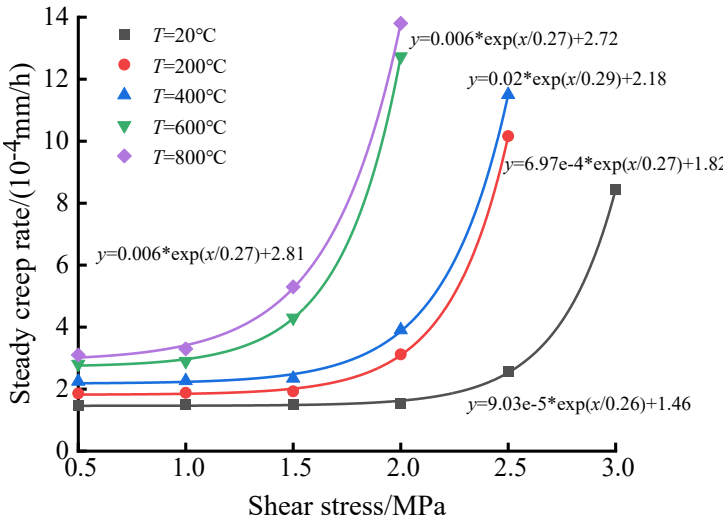


Fig. 9. Steady-state creep rate curves of the specimens under high temperatures

The relationship between creep rate and time under the final shear stress level is shown in Fig. 10. As can be observed from the figure, the creep rate first gradually decreases, then stabilizes, and finally increases abruptly, forming an approximately "U"-shaped curve. The tests demonstrate that under high temperatures, the specimens sequentially underwent decelerating creep, steady-state creep, and accelerating creep stages, with rapid failure occurring during the accelerating creep stage. Both the decelerating and accelerating creep stages were of relatively short duration, whereas the steady-state creep stage persisted for a significantly longer period. With increasing temperature, the creep rate of the specimens progressively increased, while the total creep duration gradually decreased. The total creep durations at 20°C, 200°C, 400°C, 600°C, and 800°C were 47.3h, 45.2h, 41.6h, 39.2h, and 28.8h, respectively.

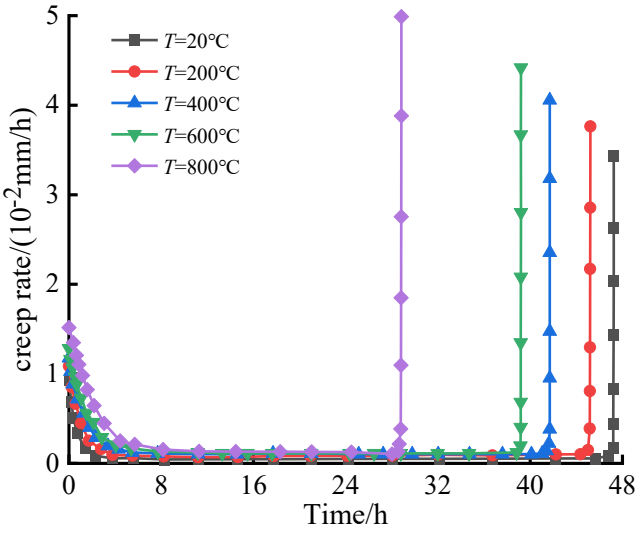


Fig. 10. Creep rate curve of the specimen under the final shear stress level

3.4 Long-term shear strength

The long-term strength of a rock mass is a critical indicator for assessing the long-term stability and safety of rock engineering projects, taking into account time-dependent effects. The long-term strength of rock is defined as the maximum sustained load that the rock can withstand without undergoing unstable deformation. When the stress level exceeds this threshold value, the rock will experience creep failure. This study determined the long-term shear strength of sandstone discontinuities under high temperatures using the steady-state creep rate method (Wang et al. 2021; Zhang et al. 2019). Taking the case of 20°C as an example, Fig. 11 shows the relationship between the steady-state creep rate and shear stress. A distinct inflection point is observed in the curve. Tangents were drawn to the curve segments before and after this inflection point, respectively. The shear stress corresponding to the intersection point A of these two tangents yields the long-term shear strength of the specimen.

Using this method, the long-term shear strengths of the specimens at 20°C, 200°C, 400°C, 600°C, and 800°C were determined to be 2.62MPa, 2.24MPa, 2.08MPa, 1.67MPa, and 1.51MPa, respectively, as shown in Fig. 12. The long-term shear strength of the specimen gradually decreases with increasing temperature. Compared to the strength at 20°C, the strengths at 200°C, 400°C, 600°C, and 800°C decreased by 14.50%, 20.61%, 36.26%, and 42.36%, respectively.

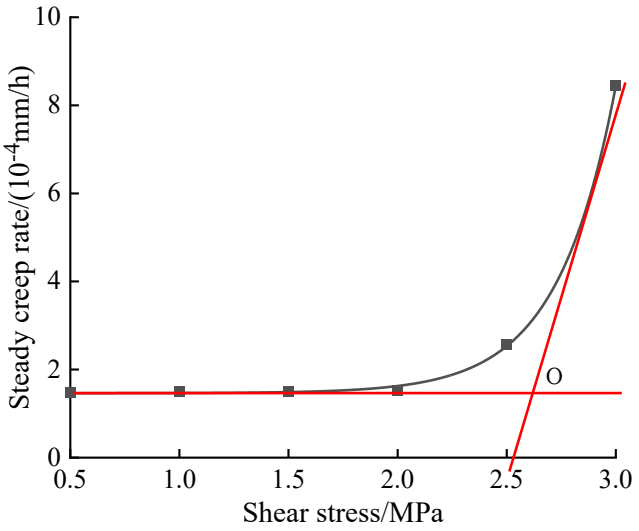


Fig. 11. Steady-state creep rate curves of the specimen under different shear stress levels (T=20°C)

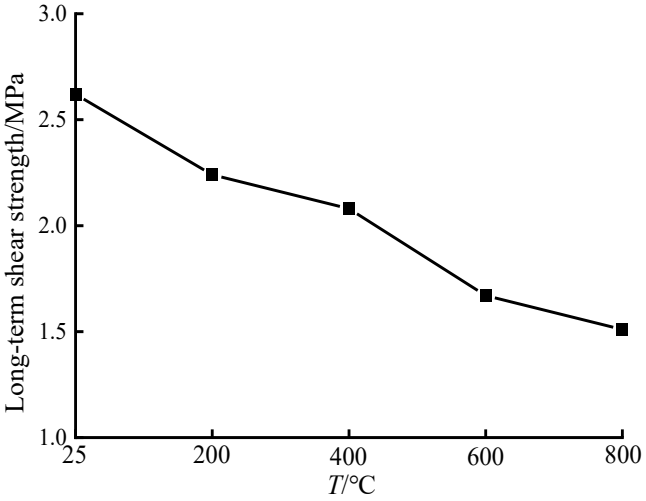


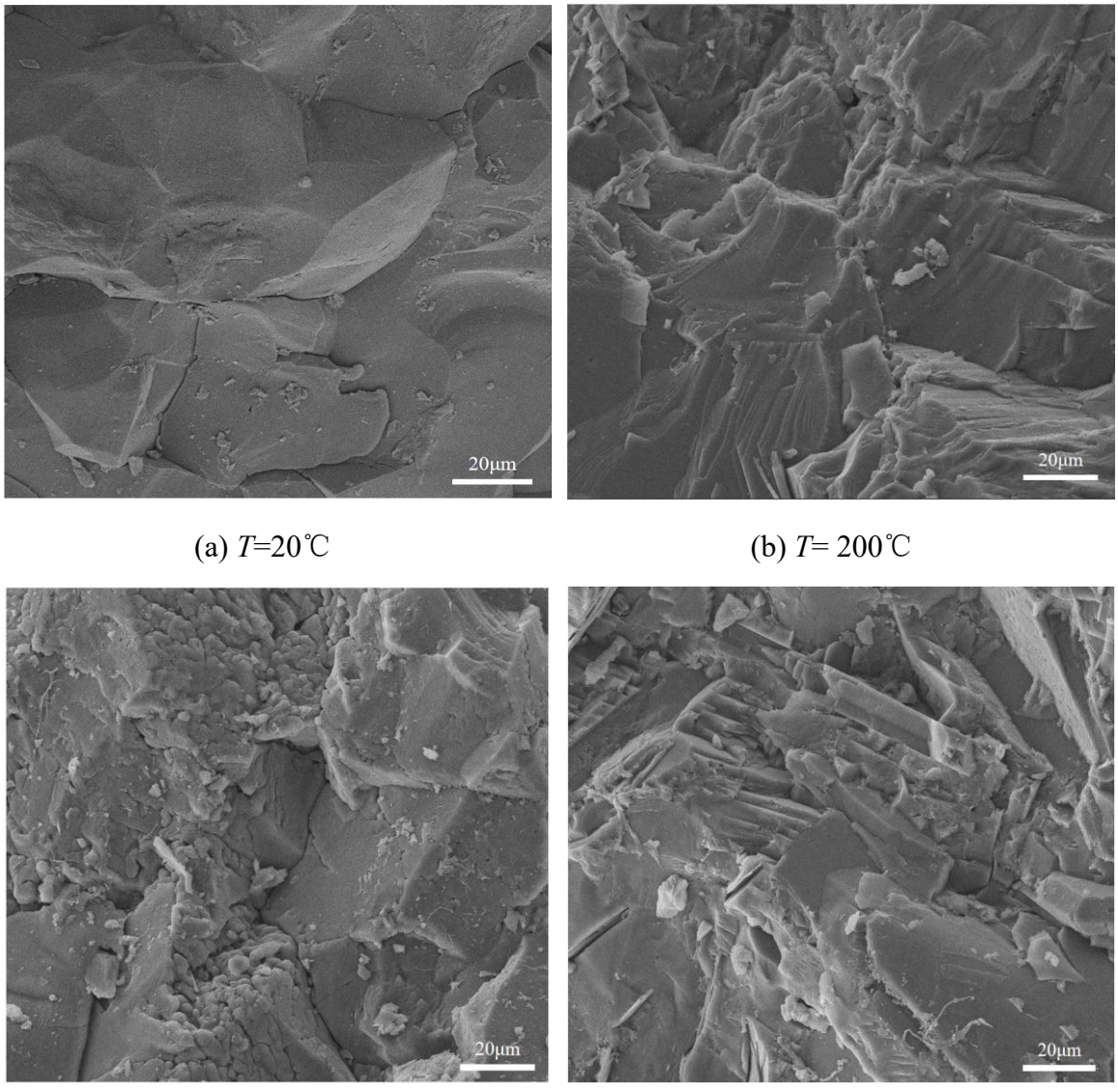
Fig. 12. Long-term shear strength of the specimen under high temperatures

4. Microscopic structural damage characteristics

4.1 SEM Analysis

To analyze the thermal damage mechanisms of sandstone discontinuities under high temperatures, SEM analysis was performed on slices taken from the central part of specimens after exposure to different temperatures. Fig. 13 presents SEM images magnified 1000 times for specimens under high temperatures. At T=20°C (Fig. 13a), the rock surface appears relatively smooth and compact. The number, length, and aperture of cracks are limited, with the microstructure dominated by micro-pores and small pores. When the temperature increases to 200°C (Fig. 13b), intergranular and transgranular cracks emerge on the rock

surface. Noticeable expansive deformation of mineral crystals occurs, accompanied by the detachment of mineral particles. At T=400°C and 600°C (Fig. 13c and 13d), the evaporation and escape of structurally bound water disrupt the mineral lattice structure, leading to the decomposition and oxidation of some minerals. The significant differential thermal expansion among various minerals, coupled with temperature gradients, generates substantial thermal stress. This results in a rapid increase in the size and number of both intergranular and transgranular cracks. The further propagation of these micro-cracks ultimately forms an interconnected fracture network.



(a) T=20℃ (b) T= 200℃

(c) T=400℃ (d) T= 600℃

Fig. 13. SEM images of the specimens under high temperatures

It can be concluded that as the temperature rises, the deterioration characteristics of the

rock, such as microcracks and pores, become increasingly pronounced. This is evidenced by a greater number of cracks, increased crack length and width (aperture), and the generation of extensive cracking on the surface. These observations indicate that the degree of thermal damage in the rock intensifies with increasing temperature.

4.2 NMR Testing

The MesoMR23-060-H-I NMR analyzer was employed to investigate the influence of high temperature on the pore structure of sandstone. Natural rock typically exhibits a multi-scale pore structure internally, where pores of different sizes possess distinct transverse relaxation times (T_2). The T_2 distribution reflects pore size information. A higher T_2 amplitude indicates a greater number of pores within the corresponding size range. Furthermore, the area under a T_2 spectral peak represents the total volume of pores, the width of a peak reflects the size distribution of specific pores, and the number of peaks indicates the multiplicity of distinct pore families. Consequently, the T_2 distribution provides a direct representation of the pore volume distribution, while the continuity of the T_2 spectrum signals characterizes the connectivity of the microscopic pore structure within the rock.

Fig. 14 shows the NMR T_2 spectrum distributions of specimens after exposure to different high temperatures. The T_2 spectrum curves of the specimens primarily exhibit two peaks, indicating that the internal pore structure of the specimens mainly consists of three size ranges. From left to right, these correspond to the distribution of small pores, medium pores, and large pores, respectively. At T=20°C, the specimen is predominantly composed of small and medium pores, with a minor proportion of large pores. As the temperature increases to 200°C and 400°C, all three spectral peaks show growth, and the overall amplitude exhibits an upward trend. This indicates that the number of pores in the sandstone specimen increases with temperature. Furthermore, the proportion of small pores decreases while the proportion of medium pores increases. This phenomenon can be attributed to the fact that high temperatures cause the development of pre-existing pores and the formation of new pores within the sandstone sample. These pores interconnect, forming larger medium-sized pores. When the temperature reaches 600°C and 800°C, the number of pores in the specimen increases significantly. The proportion of small pores continues to decline, while the proportion of large pores increases markedly. This indicates a pronounced

development of the internal pore structure, leading to the generation of more new pores. These newly formed pores subsequently expand and coalesce, forming even larger pores.

The results demonstrate that under high temperatures, the gradual growth and interconnection of micro-pores and small pores within sandstone lead to the formation of medium and large pores. This microstructural evolution is responsible for the degradation of the rock's creep mechanical properties.

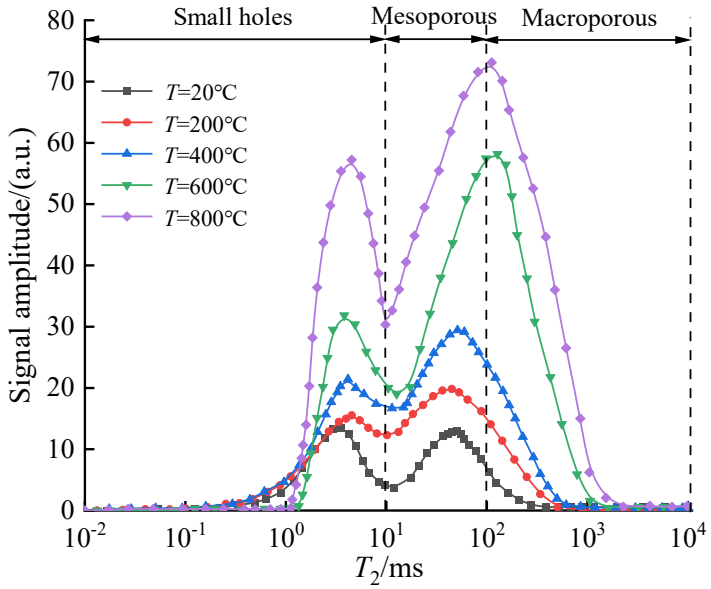


Fig. 14. T_2 spectrum distribution curves of specimens under high temperatures

4.3 Analysis of high temperature damage mechanisms

The experimental results indicate that high temperatures significantly influence the crack distribution and pore structure of the specimens, thereby affecting their creep mechanical properties. Under high temperatures, physicochemical reactions-including dehydration, thermal decomposition, quartz phase transition, mineral oxidation, chemical bond breakage, and thermal stress-occur within the mineral constituents of sandstone. These reactions lead to alterations in the internal pore structure of the rock and subsequently modify the degree of cementation between mineral particles. Higher temperatures induce more intense rock expansion, resulting in the generation of a greater number of micro-fissures within the rock. These micro-fissures continuously propagate, widen, and interconnect, ultimately leading to a progressive increase in the extent of thermal damage in the rock.

At ambient temperature, the internal structure of the sandstone specimen is compact, predominantly composed of small and medium pores, resulting in favorable creep mechanical

properties. In the temperature range of 200°C to 400°C, the evaporation and escape of internal moisture during the thermal treatment process disrupt the microstructure. Concurrently, significant differences in the thermal expansion coefficients of rock minerals generate thermal stresses between adjacent minerals, initiating microcracks. Within the specimen, small pores transform into medium pores; however, the pore structure at this stage remains dominated by small and medium pores, while overall porosity develops gradually. In terms of macroscopic mechanical properties, the creep deformation of the specimen increases progressively, and the long-term strength shows a declining trend. As the temperature further increases to the range of 400°C to 800°C, elevated thermal stresses between grains lead to a proliferation of microcracks. These microcracks interconnect and coalesce, forming a fracture network. Simultaneously, the breakage of chemical bonds (e.g., Ca-O, Al-O, K-O, Na-O) in feldspar minerals, coupled with the phase transition and volumetric expansion of quartz, further intensifies the alteration of the rock's internal structure. This causes severe damage to the microstructure of the sandstone specimen and a rapid degradation of its creep mechanical properties. The initiation, propagation, and coalescence of thermally induced cracks are identified as the primary mechanisms responsible for the temperature-dependent degradation of the creep mechanical properties observed in this study.

5. Conclusions

(1) The shear creep mechanical properties of sandstone discontinuity specimens are significantly influenced by temperature. The shear creep process primarily comprises four stages: instantaneous deformation, decelerating creep, steady-state creep, and accelerating creep. As temperature increases, the instantaneous deformation, creep deformation, and creep rate exhibit an increasing trend, whereas the creep duration, failure stress, and long-term strength show a decreasing trend. Elevated temperature intensifies slip and failure along the discontinuities, leading to continuous strength degradation and increased deformation, thereby promoting the development of nonlinear creep characteristics.

(2) SEM and NMR tests reveal that as temperature increases, the differential thermal expansion and temperature gradients among various minerals in the specimen generate greater thermal stress. This leads to an increase in the number and length of cracks, the

widening of their apertures, and their propagation into fracture networks. Furthermore, within the specimen, micro-pores and small pores gradually grow and interconnect, forming medium and large pores and progressively developing into fracture networks. This results in an increased proportion of medium and large pores and a significant rise in porosity, thereby adversely affecting the shear creep mechanical properties of the specimen.

(3) Under high temperature conditions, the specimen undergoes a series of physicochemical reactions, including dehydration, thermal decomposition, quartz phase transition, mineral oxidation, chemical bond breakage, and the development of thermal stress. These reactions induce the formation of intergranular cracks, transgranular cracks, and detachment defects among mineral particles. Higher temperatures lead to a significant increase in the number, aperture, length, and connectivity of these cracks, resulting in severe damage to the internal microstructure and a rapid degradation of the creep mechanical properties of the specimen.

Declaration of Competing Interest

The authors declare that there is no conflict of interest regarding the publication of this paper.

Data availability

Data will be made available on request.

Acknowledgments

This paper is funded by the National Natural Science Foundation of China (No.52574146); Natural Science Research of Jiangsu Higher Education Institutions of China (No. 24KJB580002 and 25KJB580002); Jiangsu Province "Qinglan Project" for Outstanding Young Teachers (No.Z302E25503).

References

Dong ZK, Li YP, Li HR, et al. Experimental Study on the Influence of Temperature on Rock Salt Creep. ROCK MECH ROCK ENG. 2023; 56(5):3499-3518. doi: 10.1007/s00603-023-03219-0

Fan LF, Yang QH, Du XL. Spalling characteristics of high-temperature treated granitic rock at different strain rates. J ROCK MECH GEOTECH. 2024; 16(4):1280-1288. doi:10.1016/j.jrmge.2023.05.016

Feng F, Zhang T, Chen SJ, et al. Analysis of failure properties of red sandstone with structural plane subjected to true triaxial stress paths. ENG FRACT MECH. 2024; 310:110490. doi:10.1016/j.engfracmech.2024.110490

Hu ZJ, Gong B, Wang QB, et al. Experimental study on shear characteristics of fiber-reinforced shotcrete-rock interface under high-and-variable temperature. ROCK MECH ROCK ENG. 2024; 57(8):6395-6420. doi:10.1007/s00603-024-03856-z

Jiang HP, Yin W, Zhang K, et al. Three-dimensional nonlinear Nishihara creep-Ubiquitous joint model considering high temperature effect. Thermal Science and Engineering Progress. 2025; 61:103528. doi:10.1016/j.tsep.2025.103528

Liang C, Liu JF, Chen ZW, et al. Study on salt rock creep characteristics of Wellbore under high temperature and high pressure. J POROUS MEDIA. 2022; 25(3):51-69. doi:10.1615/JPorMedia.2021040126

Li TB, Chen C, Peng F, et al. Creep damage constitutive model of rock based on the mechanisms of crack-initiated damage and extended damage. UNDERGR SPACE. 2024; 18:295-313. doi:10.1016/j.undsp.2023.12.008

Li XF, Wu D, Wu MX. Creep characteristics and fractional rheological model of granite under temperature and disturbance load coupling. MECH TIME-DEPEND MAT. 2024; 28(1):81-98. doi:10.1007/s11043-023-09618-8

Meng LB, Zhang S, Li TB, et al. Study on the creep constitutive model of layered rock considering anisotropic and damage factors after hightemperature exposure. INT J DAMAGE MECH. 2025; 34(3):520-541. doi:10.1177/10567895241292748

Pan XK, Chen J, Rui YC, et al. Experimental study on short-term creep crack evolution and acoustic emission characteristics of salt rock after heat treatment at different temperatures. B ENG GEOL ENVIRON. 2025; 84(5):253. doi:10.1007/s10064-025-04247-6

Pan XK, Zhou XP. Damage analysis of sandstone during the creep stage after high-temperature heat treatment based on NMR technology. ROCK MECH ROCK ENG. 2022; 55(12):7569-7586. doi:10.1007/s00603-022-03048-7

Shen YJ, Li ZY, Peng C, et al. High-temperature treated oil-rich bedded rock layer and deterioration mechanism of heat transfer performance. B ENG GEOL ENVIRON. 2025; 84(3):152. doi:10.1007/s10064-025-04154-w

Tounsi H, Rutqvist J, Hu MS, et al. Long-term sinking of nuclear waste canisters in salt formations by low-stress creep at high temperature. ACTA GEOTECH. 2023; 18(7):3469-3484. doi:10.1007/s11440-023-01900-w

Wang CP, Chen L, Liang JW, et al. Creep constitutive model for full creep process of granite considering thermal effect. ROCK SOIL MECH. 2014; 35(09):2493-2500. doi:10.16285/j.rsm.2014.09.005

Wang D, Chen GQ, Jian DH, et al. Shear creep behavior of red sandstone after freeze-thaw cycles considering different temperature ranges. B ENG GEOL ENVIRON. 2021; 80:2349-2366. doi:10.1007/s10064-020-02046-9

Xu HS, Li SJ, Xu DP, et al. Investigation on the failure mechanism of hard rock cavern subjected to adjacent structural plane based on physical model experiments. THEOR APPL FRACT MEC. 2024; 131:104447. doi:10.1016/j.tafmec.2024.104447

Xu ZH, Zhong XP, Zhang SL, et al. Experimental study on mechanical damage and creep characteristics of Gonghe granite under real-time high temperature. GEOTHERMICS. 2024; 123: 103100. doi.org:10.1016/j.geothermics.2024.103100

Yang PC, Wen J, Wenan X, et al. Experimental investigation on microstructure evolution and creep behavior of red sandstone at elevated temperature. ARCH MIN SCI. 2024; 69(3):461-483. doi:10.24425/ams.2024.151446

Yang SQ, Tang JZ, Elsworth D. Creep Rupture and Permeability Evolution in High Temperature Heat-Treated Sandstone Containing Pre-Existing Twin Flaws. ENERGIES. 2021; 14(19):6362. doi:10.3390/en14196362

Yang WD, Wang XP, Ivanovic A, et al. Coupled analytical solutions for circular tunnels considering rock creep effects and time-dependent anchoring forces in prestressed bolts. TUNN UNDERGR SP TECH. 2023; 134:104954. doi:10.1016/j.tust.2022.104954

Yu Y, Zhao GS, Ren MH. Shear mechanical properties of the interface between soil-rock mixture and rough structural plane. B ENG GEOL ENVIRON. 2024; 83(4):138. doi:10.1007/s10064-024-03625-w

Zhang QZ, Wu CZ, Fei XC, et al. Time-dependent behavior of rock joints considering asperity degradation. J STRUCT GEOL. 2019; 121:1-9. doi:10.1016/j.jsg.2019.01.004

Zhang SL, Xu SG, Xiao N, et al. Creep damage model for deep salt rock under temperature

and stress coupling effect. JOURNAL OF CHINA COAL SOCIETY. 2024; 49(08):3425-3438. doi:10.13225/j.cnki.jccs.2023.0907

Zhao CX, Lyu C, Yang MF, et al. Temperature effects on the micro-to-macro mechanical and creep properties of impurity salt rock. B ENG GEOL ENVIRON. 2025; 84(6):345. doi:10.1007/s10064-025-04291-2

Zhao JH, Jin JX, Li YF. Macro-micro failures of shear creep and creep damage model of deep hard rocks induced by initial disturbances. ENG FRACT MECH. 2025; 324:111269. doi:10.1016/j.engfracmech.2025.111269

Zhou M, He FF, Zhang WY, et al. Effect of high temperature on the mixed mode I-II fracture characteristics of hot-dry rock. ENG FRACT MECH. 2024; 303:110141. doi:10.1016/j.engfracmech.2024.110141